DETERMINATION OF α_s AND $\sin^2\theta_w$ FROM MEASUREMENTS OF THE TOTAL HADRONIC CROSS SECTION IN e^+e^- ANNIHILATION

CELLO Collaboration

H.-J. BEHREND, J. BÜRGER, L. CRIEGEE, J.B. DAINTON [1], H. FENNER, J.H. FIELD, G. FRANKE, J. FUSTER [2], Y. HOLLER, J. MEYER, V. SCHRÖDER, H. SINDT, U. TIMM, G.G. WINTER, W. ZIMMERMANN
Deutsches Elektronen-Synchrotron, DESY, D-2000 Hamburg, Fed. Rep. Germany

P.J. BUSSEY, C. BUTTAR, A.J. CAMPBELL, D. HENDRY, G. McCURRACH, J.M. SCARR, I.O. SKILLICORN, K.M. SMITH
University of Glasgow, Glasgow G12 8QQ, UK

J. AHME, V. BLOBEL, M. FEINDT, J. HARJES, M. POPPE, H. SPITZER
II. Institut für Experimentalphysik, Universität Hamburg, D-2000 Hamburg, Fed. Rep. Germany

W.-D. APEL, A. BÖHRER, J. ENGLER, G. FLÜGGE, D.C. FRIES, W. FUES, K. GAMERDINGER, P. GROSSE-WIESMANN [3], J. HANSMEYER, G. HOPP, H. JUNG, J. KNAPP, M. KRÜGER, H. KÜSTER, P. MAYER, H. MÜLLER, K.H. RANITZSCH, H. SCHNEIDER, J. WOLF
Kernforschungszentrum Karlsruhe and Universität Karlsruhe, D-7500 Karlsruhe, Fed. Rep. Germany

W. DE BOER, G. BUSCHHORN, G. GRINDHAMMER, B. GUNDERSON, Ch. KIESLING, R. KOTTHAUS, H. KROHA, D. LÜERS, H. OBERLACK, B. SACK, P. SCHACHT, G. SHOOSHTARI, W. WIEDENMANN
Max-Planck-Institut für Physik und Astrophysik, D-8000 Munich, Fed. Rep. Germany

A. CORDIER, M. DAVIER, D.FOURNIER, M. GAILLARD [3], J.F. GRIVAZ, J. HAISSINSKI, P. JANOT, V. JOURNÉ, F. LE DIBERDER, E. ROS [4], A. SPADAFORA, J.-J. VEILLET
Laboratoire de l'Accélérateur Linéaire, F-91405 Orsay Cedex, France

B. FATAH [5], R. GEORGE, M. GOLDBERG, O. HAMON, F. KAPUSTA, F. KOVACS, L. POGGIOLI, M. RIVOAL
Laboratoire de Physique Nucléaire et Hautes Energies, Université de Paris, F-75230, Paris Cedex, France

G. D'AGOSTINI, F. FERRAROTTO, M. GASPERO, B. STELLA
University of Rome and INFN, I-00185 Rome, Italy

R. ALEKSAN, G. COZZIKA, Y. DUCROS, Y. LAVAGNE, F. OULD SAADA, J. PAMELA, F. PIERRE, J. ŽAČÉK [6]
Centre d'Études Nucléaires, Saclay, F-91191 Gif-sur-Yvette Cedex, France

G. ALEXANDER, G. BELLA, Y. GNAT, J. GRUNHAUS, A. LEVY
Tel Aviv University, 69978 Ramat Aviv, Israel

0370-2693/87/$ 03.50

Received 30 October 1986

We have measured the total normalized cross section R for the process $e^+e^- \to$ hadrons at centre-of-mass energies between 14.0 and 46.8 GeV based on an integrated luminosity of 60.3 pb^{-1}. The data are well described by the standard $SU(3)_C \otimes SU(2)_L \otimes U(1)$ model with the production of the five known quarks. No open production of a sixth quark with charge 2/3 or 1/3 occurs below a centre-of-mass energy of 46.6 or 46.3 GeV, respectively. A fitting procedure which takes the correlations between measurements into account was used to determine the electroweak mixing angle $\sin^2\theta_w$ and the strong coupling constant $\alpha_s(s)$ in second-order QCD. We applied this procedure to the CELLO data and in addition included the data from other experiments at PETRA and PEP. Both fits give consistent results. The fit to the combined data yields $\alpha_s(34^2\ \mathrm{GeV}^2) = 0.165 \pm 0.030$, and $\sin^2\theta_w = 0.236 \pm 0.020$. Fixing $\sin^2\theta_w$ at the world average value of 0.23 yields $\alpha_s(34^2\ \mathrm{GeV}^2) = 0.169 \pm 0.025$.

1. Introduction

The total hadronic cross section in e^+e^- annihilation is determined by electroweak interactions and strong interactions, which can be calculated in the standard $SU(3)_C \otimes SU(2)_L \otimes U(1)$ model. The total hadronic cross section is a good quantity to determine the strong coupling constant α_s and the electroweak mixing angle $\sin^2\theta_w$, since both the cross section increase due to gluon radiation and the rise at the highest PETRA energies due to the electroweak contribution are large enough to be measurable.

The determination of α_s from the total cross section is of special interest: among all methods used so far (three-jet events, photon structure function, photon structure function, structure functions in deep inelastic scattering, and quarkonium decays), it is the only one which is not plagued by theoretical uncertainties, dependence on parton hadronization models, "higher twist" effects, large second-order corrections, or a strong renormalization scale dependence [1].

The normalized cross section R is defined as the ratio

$$R \equiv \frac{\sigma(e^+e^- \to \gamma, Z^0 \to \text{hadrons})}{\sigma(e^+e^- \to \gamma \to \mu^+\mu^-)}.$$

The $\mu^+\mu^-$ cross section is the lowest-order pointlike QED cross section of massless spin $\frac{1}{2}$ particles, and is equal to $4\pi\alpha^2/3s$, where s is the square of the centre-of-mass energy. The hadronic cross section is corrected for higher-order radiative QED graphs with photon and Z^0 exchange. At PETRA energies R is dominated by the QED one-photon annihilation process. In the quark parton model it is given by

$$R = 3\sum_f Q_f^2 , \qquad (1)$$

where the factor 3 corresponds to the number of quark colours, and where the sum runs over the quark flavours which can be produced at the relevant centre-of-mass energy, and Q_f is the electric quark charge in units of the positron charge.

QCD corrections, provided quark mass effects can be neglected, modify (1) by a factor [2]

$$1 + \alpha_s(s)/\pi + C_2[\alpha_s(s)/\pi]^2$$

$$+ \text{ higher-order corrections.}$$

Here $\alpha_s(s)$ is the "running" strong coupling constant, defined in second-order QCD as [3]

$$\sigma_s(s) = \frac{12\pi}{(33-2N_f)\log(s/\Lambda^2)}$$

$$\times\left(1 - 6\frac{153-19N_f}{(33-2N_f)^2}\frac{\log[\log(s/\Lambda^2)]}{\log(s/\Lambda^2)}\right),$$

where Λ is the QCD scale parameter. The constant

[1] Permanent address: University of Liverpool, Liverpool L69 3BX, UK
[2] On leave of absence from Inst. de Fisica Corpuscular, Universidad de Valencia, Valencia, Spain.
[3] Present address: Stanford Linear Accelerator Center, Stanford, CA94305, USA.
[4] Present address: Universidad Autónoma de Madrid, Madrid, Spain.
[5] Present address: University of Sebha, Physics Department, Libya.
[6] Present address: Nuclear Center, Charles University, CS-18000 Prague 8, Czechoslovakia.

C_2 depends on the renormalization scheme chosen to minimize the higher-order corrections. In the $\overline{\text{MS}}$ scheme [4] it is given by $C_2 = 1.986 - 0.115 N_f$. At the highest PETRA energy Z^0 exchange and, to a lesser extent, the interference between γ and Z^0 exchange become important. The prediction of the standard model, including quark mass effects, can be written as

$$R = 3 \sum_f \left(\tfrac{1}{2}\beta(3-\beta^2)\{1 + C_1^V \alpha_s(s)/\pi + C_2^V[\alpha_s(s)/\pi]^2\} C_{VV} + \beta^3\{1 + C_1^A \alpha_s(s)/\pi + C_2^A[\alpha_s(s)/\pi]^2\} C_{AA} \right), \quad (2)$$

with

$$C_{VV} = Q_f^2 - 2Q_f v_e v_f \,\mathrm{Re}(\chi(s)) + (v_e^2 + a_e^2) v_f^2 |\chi(s)|^2 ,$$

$$C_{AA} = (v_e^2 + a_e^2) a_f^2 |\chi(s)|^2 .$$

Here v and a stand for the vector and axial vector couplings of the electron and the quarks:

$$v_e = -1 + 4\sin^2\theta_w , \quad a_e = -1$$

$$v_f = +1 - \tfrac{8}{3}\sin^2\theta_w , \quad a_f = +1 \quad \text{for } f = \text{u, c}$$

$$v_f = -1 + \tfrac{4}{3}\sin^2\theta_w , \quad a_f = -1 \quad \text{for } f = \text{d, s, b}$$

and

$$\chi(s) = \frac{G_F}{8\sqrt{2}\pi\alpha} \frac{sM_Z^2}{s - M_Z^2 + iM_Z\Gamma_Z} , \quad (3)$$

with M_Z and Γ_Z being the mass and the width of the Z^0.

The dependence on finite quark masses to first order in QCD is included in eq. (3) through the threshold factors $\beta(3-\beta^2)/2$ and β^3 and the functions $C_1^V(\beta)$ [5] and $C_1^A(\beta)$ [6]. Here β is the quark velocity, and for β approaching 1, C_1^V and C_1^A approach 1. The second-order contribution has only been calculated for massless quarks. In this case, which is a good approximation at our energies, one has $C_2^A = C_2^V = C_2$. For example, at $\sqrt{s} = 14$ GeV with $\sin^2\theta_w = 0.23$ and $\Lambda_{\overline{\text{MS}}} = 610$ MeV [i.e., $\alpha_s(34^2\ \text{GeV}^2) = 0.17$], the QCD correction for massless (massive) quarks is 6.9% (8.8%) and the electroweak effects are negligible. At $\sqrt{s} = 46$ GeV, the QCD contribution to R is 5.3% independent of the quark masses, and the Z^0 exchange and the γZ^0 interference contribute 7.8% and -1.8%, respectively. These numbers are insensitive to the precise value of the Z^0 mass at present energies.

2. Detector properties and event selection

The CELLO detector was designed as a 4π detector with good detection of charged particles and photons. The main components used for this analysis are:
- the central track detector inside a superconducting solenoid ($B = 1.3$ T) of 0.5 radiation length thickness. It consists of cylindrical drift chambers interleaved with proportional chambers with cathode read-out and covers 91% of 4π;
- the cylindrical lead liquid argon calorimeter consisting of 16 modules with a thickness of 20 radiation lengths and a coverage of 87% of 4π.

A detailed description of the detector can be found elsewhere [7]. An important point for the present analysis is the long term stability of the detector components used. For example, the calibration constants for the calorimeter were stable within 1% for a data taking period of several months.

The trigger is derived from a fast pattern recognition and momentum measurement of charged particle tracks in the central detector, and from the energy deposited inside the calorimeter modules. The most important trigger required:
- at least 1 charged particle in the inner detector in coincidence with an energy deposition of at least 1.5 GeV in any one of the 16 calorimeter modules.

Additional independent triggers were:
- a purely "charged" trigger requiring at least 2 charged particles anywhere in the track detector with a transverse momentum $p_t > 200$ MeV/c. At the highest energies ($\sqrt{s} > 38$ GeV) the background conditions became worse, which required a somewhat tighter trigger: $p_t > 650$ MeV/c, and at least one pair of charged particles with a minimum opening angle of 135° in the plane transverse to the beam axis ($r\phi$);
- a purely "neutral" trigger reguiring at least 1.5 to 4 GeV shower energy deposited in any one of the 16 modules. The choice of the threshold depended on the background conditions.

Only charged particle tracks and photon showers passing the following cuts were used in the analysis:

(i) charged particles had to have a transverse momentum $p_t > 150$ MeV/c;

(ii) neutral electromagnetic showers had to have an energy $E_\gamma > 150$ MeV;

(iii) all tracks and showers had to have a polar angle with $|\cos\theta| < 0.86$;

(iv) the distance between tracks and the beam line had to be < 0.02 m in the $r\phi$ plane.

For the final multihadronic event selection we applied the following cuts:

(a) more than 4 charged particle tracks;

(b) at least 1 charged particle with a momentum $p_t > 400$ MeV/c;

(c) "visible energy" of charged particles $\Sigma|p_i| > 0.10\sqrt{s}$;

(d) "neutral energy" $\Sigma E_\gamma > 0.08\sqrt{s}$;

(e) "total energy" of all particles $\Sigma|p_i| + \Sigma E_\gamma > 0.40\sqrt{s}$;

(f) at least one opening angle between any two charged particle tracks $> 100°$ in the $r\phi$ plane;

(g) at least one negative particle.

3. Measurement of the hadronic cross section

The data were taken at centre-of-mass energies $\sqrt{s}$ between 14.0 and 46.8 GeV from 1980 to 1985. The available integrated luminosities $\mathcal{L}$ for the different energy points are shown in table 1. Part of the data were taken by varying the centre-of-mass energy in steps of 20 or 30 MeV. The continuous coverage of the energy ranges from 38.66 GeV $< \sqrt{s} <$ 38.78 GeV and 39.79 GeV $< \sqrt{s} <$ 46.78 GeV allowed a search for the bound state production of new heavy quarks, which would show up as a narrow resonance. The results of this search can be found in ref. [8]. In addition, we can exclude the open production of new heavy quarks with charge $\frac{2}{3}$ ($\frac{1}{3}$) up to a centre-of-mass energy of 46.6 (46.3) GeV. The procedure for obtaining these limits has been described in detail in ref. [8]. The limits quoted here have been improved slightly due to additional data (1 pb^{-1}) taken at $\sqrt{s} = 46.6$ GeV.

The R-value is determined by

$$R = \frac{(N_H - N_{BG})}{\mathcal{L}\epsilon_H(1+\delta_H)\sigma_{\mu\mu}},$$

where N_H and N_{BG} are the number of observed multihadron and estimated background events. $\mathcal{L}$ is the integrated luminosity, $\epsilon_H(1+\delta_H)$ is the multihadron detection efficiency. In the following we discuss these quantities and the estimates of their errors.

3.1. Background. Events from beam–gas interactions are suppressed by the cuts on the momenta (a), (b), the charge (g), and on energies (c)–(e). Events from off-momentum electrons, which convert to a multiparticle shower in a sector of the central detector are eliminated by cut (f). An upper limit of 0.1% for the remaining contribution was obtained from scanning a large fraction of the data.

Two classes of multihadronic events, produced via two photon collisions, contribute:

(1) Events with both final state leptons outside the detector acceptance are suppressed to a level of 0.2% by the cuts on the energy (c)–(e);

(2) Events from deep inelastic eγ scattering with high Q^2 may fulfill all cuts if one of the initial state leptons is scattering into the acceptance and, oppo-

Table 1
R-values and luminosities $\mathcal{L}$ from CELLO. The errors do not include uncertainties from higher-order QED radiative corrections (see text).

$\langle\sqrt{s}\rangle$ (GeV)	R ± stat. ± syst.	$\mathcal{L}$(nb^{-1})	± stat. ± syst.
14.0	4.10 ± 0.11 ± 0.11	1259	± 14 ± 25
22.0	3.86 ± 0.12 ± 0.10	2344	± 29 ± 50
33.8	3.74 ± 0.10 ± 0.10	8038	± 83 ± 172
38.3	3.89 ± 0.10 ± 0.09	8944	± 79 ± 184
41.5	4.03 ± 0.17 ± 0.10	4184	± 65 ± 86
43.5	3.97 ± 0.08 ± 0.09	21828	± 150 ± 401
44.2	4.01 ± 0.10 ± 0.08	9216	± 96 ± 151
46.0	4.09 ± 0.21 ± 0.10	3400	± 58 ± 67
46.6	4.20 ± 0.36 ± 0.10	1104	± 33 ± 22

site to it, jets are detected. Their typical contribution is $\approx 0.7\%$, as determined by visual scanning.

Pair production of $\tau^+\tau^-$ is characterized by a low charged multiplicity and a low visible energy, because at least two neutrinos leave the detector unseen. They are suppressed by the cuts (a) and (c)–(e). The remaining background was found to be smaller than 0.1% by a Monte Carlo simulation of this process. Bhabha events with the electrons interacting in the beam pipe or in the inner detector are reduced by cut (a) to a negligible amount. The total number of multihadron events after subtracting background events is 12 193.

3.2. Luminosity. The time integrated lumininosity $\mathscr{L}$ was obtained from Bhabha scattering inside the acceptance of the cylindrical calorimeter. The main criteria for the event selection were:
- at least two showers with an energy greater 0.3 E_{beam} inside $|\cos\theta| < 0.83$;
- at least one charged track points at one of the showers;
- not more than 4 charged particles;
- the acollinearity angle of the two most energetic particles has to be smaller than 20°.

The shower energy and the acollinearity angle are well measured in our detector. The energy resolution of the colorimeter can be parametrized as $5\% + 10\%/\sqrt{E}$ (with E in GeV) for showers from Bhabha events, and the spatial resolutions of the central track detector are 2 mr in $r\phi$ and 3 mr $\sin^2\theta$ in rz, while for the calorimeter they are 6 mr and 10 mr respectively. The different systematic errors on the luminosity are shown in table 2. To check the systematic error, a different acceptance cut ($|\cos\theta| < 0.85$) was made. The results agreed within 1%.

The Bhabha cross section within our acceptance was determined with the Bhabha Monte Carlo generator of Berends and Kleiss [9]. This procedure leads to an effective Bhabha cross secrion $\phi_{\text{B eff}}$ which takes into account the limited acceptance volume, losses due to the acollinearity cut, and radiative corrections up to order α^3. Electroweak contributions to Bhabha scattering at our energy are negligible, because of the dominating t-channel diagram.

The main background in Bhabha events are $e^+e^- \to \gamma\gamma$ final states, where one or both photons convert in the beam pipe or the material around it. The luminosity values given in table 1 have been corrected for this contribution (1.2%). All other background sources, e.g. cosmics, $\tau^+\tau^- \to ee$, $e\mu$ and two-photon scattering, contribute each less than 0.1%. These limits were determined by a visual inspection of subsets of the Bhabha event sample, and by a $\tau^+\tau^-$ Monte Carlo simulation.

Table 2
Systematic errors on R from CELLO: common normalization error (σ_{norm}) and systematic point to point errors (σ_{ptp}). The errors do not include uncertainties from higher-order QED radiative corrections (see text).

Source	σ_{norm} (%)	σ_{ptp} (%)
luminosity		
trigger	0.5	
selection	0.7	
acollinearity cut	0.6	
energy cut	0.4	
acceptance	0.7	0.0–1.3
calibration		0.5
tracking efficiency		0.9
	1.3	1.0–1.7
multihadrons		
trigger	0.4	
data reduction	0.7	
MC generator	0.5	
rad. corrections		
(hard bremsstrahlung	0.5	0.0–0.7
selection cuts		0.6–1.2
	1.1	0.6–1.4
total	1.7	1.2–2.2

3.3. Multihadron detection efficiency and radiative corrections. The efficiency $\epsilon_{\text{H}}(1+\delta_{\text{H}})$ was determined by generating multihadrons with the LUND Monte Carlo program [10], and passing the hadrons through a detailed simulation of the detector. ϵ_{H} is simply the ratio of MC events passing our cuts to the number of generated multihadrons, including those with initial state radiation. At $\sqrt{s} = 34$ GeV, the radiative correction factor δ_{H} contains the following contributions:
- initial state vertex corrections: 8.0%;
- vacuum polarization: $10.6 \pm 0.3\%$. The uncertainty comes mainly from the poor knowledge of the total hadronic cross section at low s. However, this uncertainty partly cancels in R, since the Bhabha cross section has a similar correction;
- initial state bremsstrahlung. Its value is strongly dependent on the maximum allowed fractional

energy of the radiated photon k_{max}. However, as k_{max} approaches 1, the $1/s$ dependence of the hadronic cross section is compensated for by the loss of efficiency for events with small remaining hadronic invariant mass. For $k_{max}=0.99$ we find $\epsilon_H \approx 0.6$ and $\delta_H=0.34$ at $\sqrt{s}=34$ GeV. The product $\epsilon_H(1+\delta_H)\approx 0.8$ is insensitive to k_{max}. For heavy quark production, k_{max} is limited by the mass of the quarks, i.e. $k_{max}=1-4m_f^2/s$. The error on R coming from the uncertainty in the heavy quark thresholds and the magnitude of the low-energy hadronic cross section was evaluated to be 0.9% (at 14 GeV) and 0.5% (above 30 GeV). We have also taken into account the initial state radiation for Z^0 exchange which lowers δ_H by 2% at the highest energies. Final state radiation from quarks can be neglected [11,12];- higher-order radiative corrections. The Lund program incorporates initial state radiative corrections up to order α^3. Tsai gives an estimate of the higher-order corrections by summing all leading logarithms [12]. Since these calculations are not complete and give correction factors at the percent level with errors of the order of the correction itself, we have not applied these corrections to the data. We will indicate later by how much the results change if such a correction is applied.

The largest contribution to the detection inefficiency comes from the fact that we limited our acceptance to the central detector ($|\cos\theta|<0.86$) for three reasons:

- in the endcap region the efficiency calculations are more delicate because of the smaller number of chambers in the acceptance;
- the background from $\gamma\gamma$ collisions and beam–gas scattering is smaller in the central region;
- the angular distribution of hadrons is well described by the Monte Carlo, so extrapolating to the full solid angle can be done reliably. Fig. 1 shows the angular distribution of the sphericity axis, corrected for QED and gluon radiation effects, and detector efficiency. The solid line is the result of a fit of $1+a\cos^2\theta$ which gives $a=1.00\pm0.01$, as expected for the pair production of massless spin $\frac{1}{2}$ particles. The uncertainty on the efficiency due to the error on a is negligible.

Further inefficiencies arise from the multiplicity and energy cuts. Fig. 2 shows these distributions for Monte Carlo events and a data sample at $\sqrt{s}=43.6$ GeV, selected by cuts looser than the final ones. The

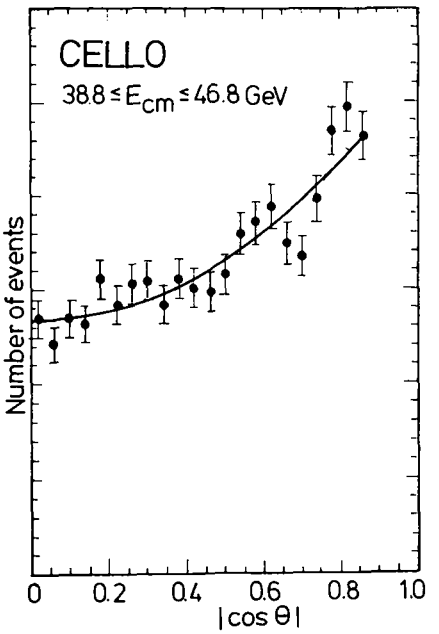

Fig. 1. Angular distribution of the corrected sphericity axis. The solid line corresponds to a fit of $1+a\cos^2\theta$ with $a=1.00\pm0.01$.

inefficiency is determined by the fractional area below the cut values. The measured distributions are in fair agreement with the Monte Carlo ones. Small relative displacements of the Monte Carlo and the

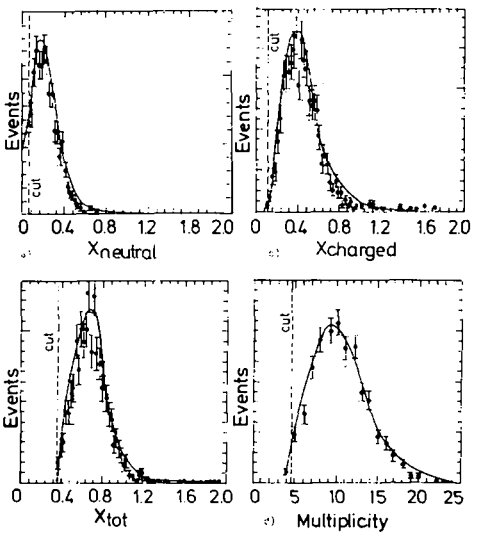

Fig. 2. Comparison between data and Monte Carlo. (a) Neutral energy fraction. (b) Charged energy fraction. (c) Total visible energy fraction. (d) Charged multiplicity.

experimental distributions were corrected by shifting the Monte Carlo distributions so that the mean values coincided. Since the total displacements and the area below the cut value are both small, the total systematic error from this procedure is also small. The systematic uncertainties due to this procedure were estimated from the variation in the area below the cut value obtained by the maximum acceptable displacement of the Monte Carlo distribution. This was done for each distribution separately. The largest error comes from the neutral energy distribution.

We found the inefficiency to be independent of the specific fragmentation scheme, provided the models were tuned for optimal agreement with the data. For example, if we switch from string fragmentation to independent fragmentation with the parameters described in a previous publication [13], we find that ϵ_H changes by less than 0.1%. The tuning of the different models required rather different values of α_s [13], which was found to influence the determination of ϵ_H more than the choice of model itself. If we change α_s by 20% around the fitted value, ϵ_H changes by 0.2%.

We assign no systematic error to the background subtraction, because the contributions remaining after applying all cuts and removing obvious background events are negligible. For the determination of R the various systematic errors on ϵ_H, δ_H, and $\mathcal{L}$ are combined quadratically and total 2.1–2.8%. These errors do not include the uncertainty from higher-order radiative corrections, as discussed above. Table 2 summarizes the different contributions and their splitting into point to point and common normalization errors. The results on R for different centre-of-mass energies are given in table 1 together with the corresponding luminosities.

3.4. Cross-check on systematic errors. The systematic errors were cross-checked by an independent analysis of part of the data using charged particles only [8,14]. The luminosity was determined independently too. The difference in the R-values was consistent with the errors discussed above. For part of the data the luminosity was also determined using the endcap calorimeter. It was found to be in good agreement with the quoted luminosity.

4. Determination of α_s and $\sin^2\theta_w$

The parameters $\lambda_{\overline{MS}}$ or (α_s for fixed s) and $\sin^2\theta_w$ can be determined by fitting eq. (2) to the data. Since the data points at the different centre-of-mass energies are not completely independent, we have used the following procedure to take the correlations of the individual data point errors into account.

4.1. Method. One defines an $n\times n$ error matrix V_{ij} for n measurements. The diagonal elements are given, for each measurement, by the sum of the squares of the statistical σ_{stat}, systematic point to point σ_{ptp}, and common normalization error σ_{norm}. The correlation between data points i and j is contained in the off-diagonal matrix element V_{ij}, which is estimated by the product of σ^i_{norm} of measurement i and σ^i_{norm} of measurement j. The expression to be minimized is then

$$\chi^2 = \Delta^T V^{-1} \Delta .$$

Here Δ is the vector of the n residuals $R_i - R_{fit}$. If the off-diagonal elements V_{ij} are all zero, χ^2 reduces to the usual expression for independent measurements. In this method all data points are handled in a symmetric way, so one can easily introduce different normalization errors for different running periods or introduce correlations between different experiments, e.g. coming from uncertainties in radiative corrections. In previous determinations of α_s from R measurements [15–17] a normalization constant f was fitted as a free parameter to take the correlations into account: $\chi^2 = (f-1)^2/\sigma_n^2 + \sum (fR_i - R_{fit})^2/(f\sigma_i)^2$, where σ_n is the relative common normalization error and $\sigma_i^2 = \sigma_{stat}^2 + \sigma_{ptp}^2$. If the combined data from different experiments are to be fitted with this method, one has to introduce one or more free normalization parameters for each experiment (in the data to be discussed hereafter up to 10). With the matrix method one fits only the two physical parameters and various correlations can be studied in a simple way.

4.2. Results. From a fit to the CELLO data we obtain

$$\alpha_s(34^2\ \mathrm{GeV}^2) = 0.19 \pm 0.05 ,$$

$$\sin^2\theta_w = 0.20 \pm 0.03 \quad (\chi^2/\mathrm{dof} = 3/7) .$$

The data and their statistical and total systematic errors as well as the fit are shown in fig. 3a. As mentioned, the variation of α_s as a function of s was taken into account. We have chosen $s = 34^2$ GeV^2 as reference, as for our previous α_s determination [13]. We

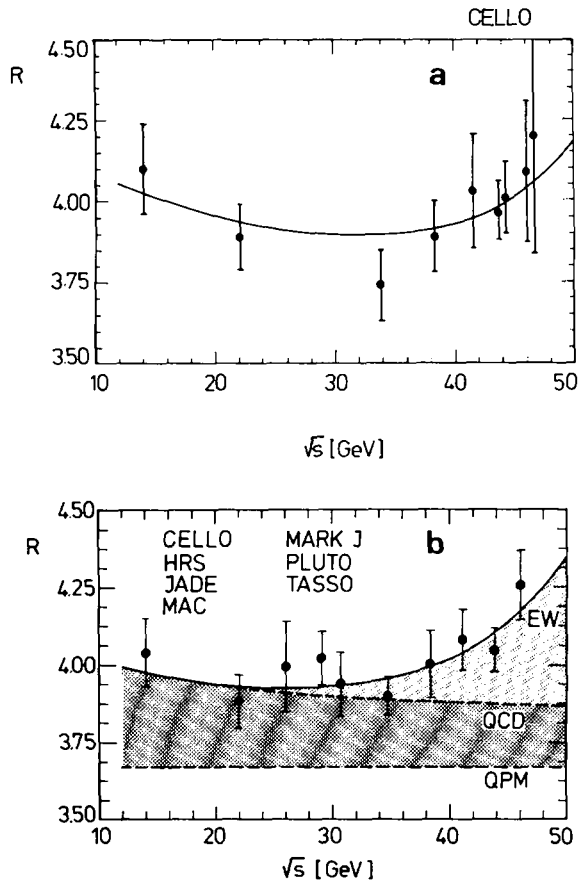

Fig. 3. Measured R values and best fit (solid line) (a) for the CELLO data, and (b) for the combined data of PEP and PETRA experiments. The errors include both statistical and common normalization errors (see text). The dashed lines indicate the quark parton model (QPM) and the QCD contributions.

used $M_Z = 92.3$ GeV/c^2 [18] and $\Gamma_Z = 2.5$ GeV/c^2; the results for the fitted parameters are insensitive to these values. With our parametrization of $\chi(s)$, the one-loop corrections to the Z^0 propagator have a negligible effect on the value of $\sin^2\theta_w$ [19]. The fitted value of the weak mixing angle $\sin^2\theta_w$ is in good agreement with the world average of 0.23, which has been determined in completely different processes: neutrino scattering [20], the masses of the weak gauge bosons [18], polarized electron–deuteron scattering [21], and asymmetries in lepton pair production [22]. If we impose $\sin^2\theta_w = 0.23$, we get for the strong coupling constant from the CELLO data

$$\alpha_s(34^2\ \text{GeV}^2) = 0.16 \pm 0.05\,,$$

consistent with previous CELLO measurements [13].

To reduce the error, we use this procedure to fit the data from all experiments at PEP [23,24] and PETRA [15–17,25]. In order to do this properly, the R-values and errors used all have to have the same meaning. Radiative corrections involving Z^0 exchange (up to 2% in the PETRA energy range) have been made by CELLO, MAC [24], and MARK J [16], but had to be applied to all other experiments. Higher-order QED corrections have been applied so far only by MAC, who also quote an R-value without this correction which we have used. TASSO [17] includes in the common normalization error an estimate of the higher-order radiative correction of 2%, which we have taken out. The covariance matrix for all experiments is formed in a similar way as described above for a single experiment. However, some experiments give slightly different normalization errors for different running periods. In this case the errors are split into a common normalization error for all running periods (σ_{norm1}), while for the running period concerned the normalization error σ_{norm2} is added quadratically to yield the correct total normalization error. These errors are indicated in table 3. It might be assumed that the hard QED bremsstrahlung correction with its dependence on the hadronic cross section at small s, provides a correlation between the R-values of the various experiments. However, in the calculation of R the product of the correction and the acceptance enter, and the latter is quite detector dependent. Therefore we have assumed no correlation between experiments in all our fits (all corresponding off-diagonal elements V_{ij} are 0), but we will indicate below the effect of such a hypothetical correlation on the final results. The R-values and errors from the PEP and PETRA experiments used in the fit are given in table 3. We obtain from the fit [‡1]

$$\alpha_s(34^2\ \text{GeV}^2) = 0.165 \pm 0.030,$$

$$\sin^2\theta_w = 0.236 \pm 0.020 \quad (\chi^2/\text{dof} = 51/61)\,.$$

[‡1] The fitting program finds also a second minimum with $\alpha_s = 0.19 \pm 0.03$ and $\sin^2\theta_w = 0.56 \pm 0.02$. This solution is characterized by a large negative interference term and a large positive direct Z^0 exchange and will not be considered further here, since this value of $\sin^2\theta_w$ is ruled out by other measurements [18].

Table 3
R-values used in the fit. If the point to point error σ_{ptp} is not given, it is included in the statistical error. If a second normalization error σ_{norm2} is given, it has to be added in quadrature to the first one. Note that for some experiments small corrections to published values have been made (see text).

Experiment	$\sqrt{s}$	R	σ_{stat} (%)	σ_{ptp} (%)	σ_{norm1} (%)	σ_{norm2} (%)
HRS	29.00	4.20	0.8		7.0	
MAC	29.00	4.00	0.8		2.1	
CELLO	14.04	4.10	2.6	2.2	1.7	
	22.00	3.86	3.0	2.1	1.7	
	33.80	3.74	2.6	1.9	1.7	
	38.28	3.89	2.6	1.7	1.7	
	41.50	4.03	4.1	1.8	1.7	
	43.60	3.97	2.0	1.4	1.7	
	44.20	4.01	2.5	1.2	1.7	
	46.00	4.09	5.1	1.9	1.7	
	46.60	4.20	8.5	1.7	1.7	
JADE	14.04	3.94	3.6		2.4	
	22.00	4.11	3.2		2.4	
	25.01	4.24	6.8		2.4	
	27.66	3.85	12.5		2.4	
	29.93	3.55	11.3		2.4	
	30.38	3.85	4.9		2.4	
	31.29	3.84	7.3		2.4	
	33.89	4.17	2.4		2.4	
	34.50	3.94	5.1		2.4	
	35.01	3.94	2.5		2.4	
	35.45	3.94	4.6		2.4	
	36.38	3.72	5.7		2.4	
	40.32	4.07	4.7		2.4	0.9
	41.18	4.24	5.2		2.4	0.9
	42.55	4.24	5.2		2.4	0.9
	43.53	4.05	5.0		2.4	0.9
	44.41	4.04	5.0		2.4	0.9
	45.59	4.47	5.0		2.4	0.9
	46.47	4.11	5.9		2.4	0.9
MARK J	22.00	3.66	2.2	3.0	2.1	
	25.00	3.89	5.4	3.0	2.1	
	30.60	4.09	3.4	3.0	2.1	
	33.82	3.71	1.6	3.0	2.1	
	34.63	3.74	0.8	3.0	2.1	
	35.11	3.85	1.6	3.0	2.1	
	36.36	3.78	4.0	3.0	2.1	
	37.40	3.97	9.3	3.0	2.1	
	38.30	4.16	2.2	3.0	2.1	
	40.36	3.75	4.0	3.0	2.1	
	41.50	4.32	4.6	3.0	2.1	
	42.50	3.85	5.2	3.0	2.1	
	43.58	3.91	1.5	3.0	2.1	
	44.23	4.14	1.9	3.0	2.1	
	45.48	4.17	4.8	3.0	2.1	
	46.47	4.35	3.9	3.0	2.1	

Table 3 (continued)

Experiment	$\sqrt{s}$	R	σ_{stat} (%)	σ_{ptp} (%)	σ_{norm1} (%)	σ_{norm2} (%)
PLUTO	27.60	4.07	7.1		6.0	
	30.80	4.11	3.2		6.0	
TASSO	14.00	4.14	7.3		3.5	2.0
	22.00	3.89	4.4		3.5	2.0
	25.00	3.72	10.2		3.5	2.0
	33.00	3.74	7.2		3.5	2.0
	34.00	4.14	3.1		3.5	2.0
	35.00	4.23	2.1		3.5	2.0
	27.50	3.91	8.2		3.5	2.0
	30.10	3.94	4.6		3.5	2.0
	31.10	3.67	4.9		3.5	2.0
	33.20	4.49	6.3		3.5	2.0
	34.00	4.10	4.9		3.5	2.0
	35.00	4.04	4.2		3.5	2.0
	36.10	3.94	4.3		3.5	2.0
	41.50	4.11	2.9		3.5	3.0
	44.20	4.28	3.8			3.0

The averaged data, including the statistical and total systematic errors and their correlations are shown in fig. 3b together with the fit. Also indicated are the prediction of the quark–parton model and the contribution from the QCD corrections. The decrease with energy in the QCD contribution is due to the "running" of α_s. We have checked the consistency of the various experiments by fitting the normalization of each experiment with the best values of α_s and $\sin^2\theta_w$ from the combined fit. The fitted normalization factors are consistent with the quoted systematic errors.

The separation of the systematic errors into point to point and overal normalization errors for an experiment is subject to some degree of uncertainty. We therefore performed the fit for different assumptions on the splitting of the systematic errors into point to point errors and normalization errors. The results and errors turn out to be rather insensitive to this splitting, although the degree of correlation between the errors on α_s and $\sin^2\theta_w$ does depend on it, as is shown in fig. 4 for three cases: (a) the best estimate for the splitting of the errors as used for the above results (solid line); (b) all off-diagonal elements decreased by 50% (dotted line); (c) all off-diagonal elements increased by 50% (dashed line). Note that the total error always stays constant, only the amount of correlation is changed, yielding α_s values between 0.162 and 0.167, which is well within the total systematic error. The correlation between α_s and $\sin^2\theta_w$ is -0.49 for (a). These fits assume, as explained above, that there is no common systematic error in all the experiments. If we introduce a hypothetical common error of 1% in R, keeping the total error constant, α_s changes by -0.007 and $\sin^2\theta_w$ by -0.005, and their errors increase by 0.005 and 0.001, respectively.

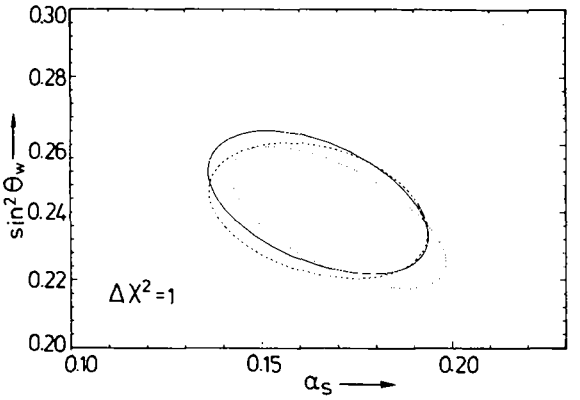

Fig. 4. Error contours corresponding to the standard model fit for three different assumptions on the splitting of the systematic error into point to point and common normalization error (see text).

The value for $\sin^2\theta_w$ is in good agreement with the world average of 0.23. In fig. 3b the rise in R from the electroweak effects at the highest PETRA energies is clearly observed. To estimate the statistical significance of this rise, the data are grouped into a "low"-energy region from 14 to 37 GeV and into a high-energy region beyond. The difference between the high-energy R-values and the extrapolation of a fit to the lower-energy points, excluding electroweak effects, are then computed using the full covariance matrix. The probability that the high-energy points of PETRA are a continuation of the low-energy ones is found to be 10^{-3}.

If we fix $\sin^2\theta_w$ to the world average of 0.23, we get for the strong coupling constant [12]

$$\alpha_s(34^2\ \mathrm{GeV}^2) = 0.169 \pm 0.025\ .$$

The determination of α_s from R is independent of uncertainties and ambiguities at the parton and fragmentation level, which are a major source of the large systematic errors in previous determinations of α_s from topological quantities [1,13]. The above value of α_s corresponds to $\Lambda_{\overline{\mathrm{MS}}} = 610^{+470}_{-340}$ MeV. In QCD α_s is expected to vary as function of energy. We have searched for evidence of this running by parametrizing the QCD term by a linear energy dependence $[a + b(\sqrt{s} - 34\ \mathrm{GeV})]$ and fitting this to the data using a constant $\sin^2\theta_w$ of 0.23. We find $b = (-0.75 \pm 0.73) \times 10^{-3}\ \mathrm{GeV}^{-1}$, which implies an 85% probability for α_s to run in the right direction, i.e. $b < 0$, with a slope compatible with the QCD expectation ($b \simeq -1.3 \times 10^{-3}\ \mathrm{GeV}^{-1}$). The parameter a, which is a theory independent parametrization of the QCD contribution to R at 34 GeV, was found to be 1.062 ± 0.011 and uncorrelated with b.

As mentioned before, higher-order QED corrections have not been calculated completely and although the corrections to Bhabha scattering and hadron production partially cancel in the ratio R, the remaining contribution is estimated to be at the per-cent level. A reduction of all R values by 1% yields $\alpha_s = 0.145 \pm 0.024$. Therefore it is important to calculate these higher-order corrections more accurately, since they imply errors on the same level as the experimental errors.

The data from PEP and PETRA can also be used to look for deviations from pointlike interactions by modifying eq. (2) by a form factor:

$$R' = R\,|\,[1 \mp s/(s - \Lambda_\pm^2)]\,|^2\ .$$

Fixing $\sin^2\theta_w$ at 0.23, and varying α_s between 0.15 and 0.20, we find for the cut-off parameters at the 95% confidence level: $\Lambda_+ > 384$ GeV and $\Lambda_- > 378$ GeV. These values do not differ significantly from those quoted by single experiments [15–17], since we took the error from α_s into account in the fit.

5. Conclusion

We have measured the total hadronic cross section in the energy range $14.0 < \sqrt{s} < 46.8$. The data are well described by the production of the five known quarks. No production of a sixth quark with charge $\frac{2}{3}$ or $\frac{1}{3}$ occurs below a centre-of-mass energy of 46.6 or 46.3 GeV, respectively. From these measurements we have determined the electroweak mixing angle $\sin^2\theta_w$ and the strong coupling constant α_s using a fit procedure which takes correlated errors into account.

The $\sin^2\theta_w$ determination from the combined data of the PEP and PETRA experiments has reached a precision of about 10%, which is similar to that from the asymmetry measurements of purely leptonic final states in e^+e^- annihilation [22]. Of course, neutrino scattering [20] and the determination of the gauge boson masses [18] have provided more accurate measurements of $\sin^2\theta_w$, but its determination from R is an independent test of the standard model.

The importance of the determination of α_s from R stems from the fact that R is an inclusive quantity, which does not depend on the event topology and is therefore insensitive to the way the partons hadronize. From a theoretical point of view, the perturbative QCD calculation for R is noncontroversial and its dependence on the renormalization scheme (or scale) is negligible. Also "higher twist" corrections are negligible at our energies [1]. Using a method, which correctly treats systematic errors, and combining the results from various experiments, we find $\alpha_s(34^2\ \mathrm{GeV}^2)$ to be 0.169 with a total error less than

[12] We prefer to restrict our fit to a region free of resonances, although QCD is expected to describe the continuum below open $b\bar{b}$ production too (apart from resonance effects). If we include lower-energy data from CESR [26] and DORIS [27] above 7.3 GeV [excluding the Y resonances and the data above the Y(4S)] and keep $\sin^2\theta_w$ fixed at 0.23, we find $\alpha_s(34^2\ \mathrm{GeV}^2) = 0.166 \pm 0.023$ in good agreement with the result from the PEP and PETRA data.

15%, if we exclude the theoretical uncertainty from higher-order QED radiative corrections, which could lower α_s by a similar amount.

We gratefully acknowledge the outstanding efforts of the PETRA machine group which made possible these measurements. We are indebted to the DESY computer centre for their excellent support during the experiment. We acknowledge the invaluable effort of many engineers and technicians from the collaborating institutions in the construction and maintenance of the apparatus, in particular the operation of the magnet system by M. Clausen, P. Röpnack, and the cryogenic group. We thank Dr. K.H. Pape for his assistance with our IBM emulator. We are grateful to Dr. W. Hollik for discussions on radiative corrections and to Dr. D. Haidt for a critical reading of the manuscript. The visiting groups wish to thank the DESY Directorate for the support and kind hospitality extended to them. This work was partially supported by the Bundesministerium für Forschung und Technologie (Germany), the Commissariat à l'Energie Atomique and the Institut National de Physique Nucléaire et de Physique des Particules (France), the Science and Engineering Research Council (UK), and the Israeli Ministry of Science and Development.

References

[1] D.W. Duke and R.G. Roberts, Phys. Rep. 120 (1985) 275.
[2] M. Dine and J. Sapirstein, Phys. Rev. Lett. 43 (1979) 668;
K.G. Chetyrkin et al., Phys. Lett. B 85 (1979) 277;
W. Celmaster and R.J. Gonsalves, Phys. Rev. Lett. 44 (1980) 560.
[3] W.E. Caswell, Phys. Rev. Lett. 33 (1974) 244;
D.R.T. Jones, Nucl. Phys. B 75 (1974) 531;
A.A. Belavin and A.A. Migdal, JETP Lett. 19 (1974) 181.
[4] W.A. Bardeen et al., Phys. Rev. D 18 (1978) 3998.
[5] T.W. Appelquist and H.D. Politzer, Phys. Rev. Lett. 34 (1975) 43; Phys. Rev. D 12 (1975) 1404;
A. De Rujula and H. Georgi, Phys. Rev. D 13 (1976) 1296.
[6] J. Jersak et al., Phys. Rev. D 25 (1982) 1219;
S. Güsken et al., Phys. Lett. B 155 (1985) 185.
[7] CELLO Collab., H.-J. Behrend et al., Phys. Scr. 23 (1981) 610.
[8] CELLO Collab., H.-J. Behrend et al., Phys. Lett. B 144 (1984) 297.
[9] F.A. Berends and R. Kleiss, Nucl. Phys. B 228 (1983) 537.
[10] B. Andersson et al., Z. Phys. C 6 (1980) 235; Nucl. Phys. B 197 (1982) 45;
T. Sjöstrand, Comput. Phys. Commun. 27 (1982) 243; 28 (1983) 229.
[11] T. Kinoshita, J. Math. Phys. 3 (1962) 650;
T.D. Lee and M. Nauenberg, Phys. Rev. 133 (1964) 1549.
[12] Y.S. Tsai, SLAC report PUB-3129 (1983), unpublished.
[13] CELLO Collab., H.-J. Behrend et al., Phys. Lett. B 138 (1984) 311.
[14] CELLO Collab., Y. Lavagne, Ph. D. thesis, Saclay (1986).
[15] JADE Collab., W. Bartel et al., Phys. Lett. B 129 (1983) 145; B 160 (1985) 337;
JADE Collab., B. Naroska, DESY Report 86-113 (1986), Phys. Rep., to be published.
[16] MARK J Collab., B. Adeva et al., Phys. Rev. D 34 (1986) 681;
MARK J Collab., D. Linnhöfer, Ph.D. thesis, Aachen (1986).
[17] TASSO Collab., R. Brandelik et al., Phys. Lett. B 113 (1982) 499;
TASSO Collab., M. Althoff et al., Phys. Lett. B 138 (1984) 441; and private communication.
[18] Particle Data Group, M. Aguilar-Benitez et al., Review of Particle Properties, Phys. Lett. B 170 (1986) 78;
UA1 Collab., G. Arnison et al., Phys. Lett. B 166 (1986) 484;
UA2 Collab., C. Gössling, Proc. XVIIth Intern. Symp. on Multiparticle dynamics (Austria, 1986), ed. M. Markytan, to be published.
[19] W. Hollik, DESY report 86-049 (1986); and private communication.
[20] CCCFRR Collab., P.G. Reutens et al., Phys. Lett. B 152 (1985) 404;
CDHS Collab., A. Abramowicz et al., Phys. Rev. Lett. 57 (1986) 298;
CHARM Collab., J.V. Allaby et al., Phys. Lett. B 177 (1986) 446;
FFMM Collab., D. Bogert et al., Phys. Rev. Lett. 55 (1985) 1969.
[21] C.Y. Prescott et al., Phys. Lett. B 84 (1979) 524.
[22] W. de Boer, MPI-PAE/Exp. El. 167, in: Proc. XVIIth Intern. Symp. on Multiparticle dynamics (Austria, 1986), ed. M. Markytan, to be published;
B. Naroska, DESY Report 86-051 (1986), in: Proc. XXIst Rencontre de Moriond, (Les Arcs, 1986), ed. Tran Thanh Van, to be published.
[23] HRS Collab., D. Bender et al., Phys. Rev. D 31 (1985) 1.
[24] MAC Collab., E. Fernandez et al., Phys. Rev. D 31 (1985) 1537.
[25] PLUTO Collab., L. Criegee and G. Knies, Phys. Rep. 83 (1982) 153.
[26] CLEO Collab., R. Giles et al., Phys. Rev. D 29 (1984) 1285;
CUSB Collab., E. Rice, Ph.D. thesis, Columbia University (1982).
[27] DASP2 Collab., S. Weseler, Diploma thesis, University of Heidelberg (1981);
DASP2 Collab., H. Albrecht et al., DESY Report 82-037 (1982), unpublished;
DESY Hamburg–Heidelberg–MPI Munich Collab., P. Bock et al., Z. Phys. C 6 (1980) 125;
LENA Collab., B. Niczyporuk et al., Z. Phys. C 15 (1982) 299;
PLUTO Collab., C. Berger et al., Phys. B 81 (1979) 410;
PLUTO Collab., Ch. Gerke, Dissertation, University of Hamburg (1979).